Abstract

Base station antenna arrays are a promising method for providing large capacity increases in cellular mobile radio systems. This article considers channel-modeling issues, receiver structures, and algorithms, and looks at the potential capacity gains that can be achieved.

Smart Antenna Arrays for CDMA Systems

JOHN S. THOMPSON, PETER M. GRANT, AND BERNARD MULGREW

Wireless communications have become a significant area of growth within the last few years. There are a diverse range of products and services currently on the market, but cellular or personal communications services (PCS) radio networks probably have the highest public profile. These services provide highly mobile, widely accessible two-way voice and data communications links [1]. In general, the most complex and expensive part of the radio path for these systems is the base station. As a result, manufacturers have been designing networks that have high efficiency in terms of the bandwidth occupied and the number of users per base station [2]. This trend has been at the expense of high-power transmitters and receivers which employ very computationally expensive signal processing techniques.

The second generation of cellular telephones, based on digital signaling and time and frequency division multiple access, have recently been introduced round the world. Typical examples include the European Global System for Mobile Telecommunications (GSM) and the North American IS-54 access protocols [3]. However, there is also considerable interest in code division multiple access (CDMA) techniques for cellular systems [4]. The IS-95 standard for CDMA cellular systems was published in 1992; there is also interest in CDMA systems for the U.S. 1.9 GHz PCS bands [5] and the European third-generation universal mobile telephone system (UMTS) [6].

Whatever the relative merits of a given cellular system, it seems that considerable system capacity gains are available from exploiting the different spatial locations of cellular users [7]. There are a number of methods to achieve this, from simple sectorization schemes [8] to complex adaptive antenna array techniques [9]. This article will consider antenna arrays for the mobile-to-base-station or reverse link of a CDMA cellular system. It begins with an introduction to CDMA communications systems and also addresses the general topic of antenna array receivers. Channel modeling is then discussed, because this will influence the design of CDMA receivers. The specific form of receiver algorithms will then be discussed, and some performance comparisons are provided. Finally, the most important question for implementing antenna array systems is what capacity gains are achievable. Some simple analysis is presented to provide an initial answer.

Direct-Sequence CDMA

CDMA techniques are based on spread spectrum communications, which were originally developed for military applications. A simple definition of a spread spectrum signal is that its transmission bandwidth is much wider than the bandwidth of the original signal [10]. There are a number of ways to achieve this, but this article will focus on direct-sequence spread spectrum techniques, which are used in IS-95-based systems.

The reverse links for all users within a CDMA system can be conducted over the same radio frequency (RF) bandwidth so that complete frequency reuse for that link is obtained throughout all cells [4]. To distinguish one user's transmission from another, each mobile modulates the voice data symbols by a pseudo-noise (PN) code. Each symbol is composed of W binary "chips" which have a much shorter period than that of the original data symbols, so the signal bandwidth is considerably increased. The generic form of the reverse link for a binary phase shift keying (BPSK) spread spectrum system, using noncoherent detection at the receiver is shown in Fig. 1a. A PN code $c(t)$, such as that shown in Fig. 1b, is used to modulate the baseband data $x(t)$ and the resulting signal transmitted to the base station. The receiver employs noncoherent quadrature demodulation to recover the signal amplitude and phase. This signal is correlated with the PN code to provide a delayed estimate of the transmitted data $\hat{x}(t - t_d)$, where t_d denotes the time delay. A typical PN code auto-correlation function observed at the correlator output is shown in Fig. 1c: it takes on significant values only within one chip of the code arrival time.

The reverse link of a CDMA system such as that specified by IS-95 has a number of essential characteristics for effective multiple access communication. A detailed introduction to spread spectrum and CDMA techniques can be found in [11–13], but here only points relevant to this discourse will be addressed.

Spread Spectrum Bandwidth – The chip rate of the spread spectrum signal is an important parameter, and is inversely proportional to the chip period t_c. A number of different chip rates have been proposed for such systems, but a chip period of approximately 800 ns (chip rate 1.25 MHz) will be assumed for this article. Such a system is often called *narrowband* CDMA, because the baseband bandwidth is much smaller than the RF carrier frequency, which is usually at least 900 MHz for cellular systems.

Modulation Scheme – The reverse link of an IS-95 system employs 64-ary orthogonal data modulation, transmitted using offset quadrature phase shift keying (QPSK) [11]. This article will be concerned with assessing general trends rather than providing specific results for different cellular systems. So, for simplicity, a system employing differential phase shift keying (DPSK) modulation will be considered [14].

1070-9916/96/$05.00 © 1996 IEEE

Multipath Diversity – In urban areas, multipath propagation is common, whereby the receiver observes a large number of copies of the transmitted signal, each with a different time delay. The noise-like autocorrelation function of a PN code, shown in Fig. 1c, means that the correlator receiver can resolve multipath components which are spaced by 1 chip period up to the symbol period. This provides a form of multipath diversity, which can be exploited by using a RAKE receiver at the output of the code correlators [15].

Asynchronous Operation – The reverse link of a CDMA system is usually asynchronous, in the sense that the arrival times for each user's code are different. This means that the receiver for each user will observe interference from all other users in the system, since the transmitted codes will not be orthogonal. Hence, the number of users that can be simultaneously accommodated in one cell is *interference-limited*.

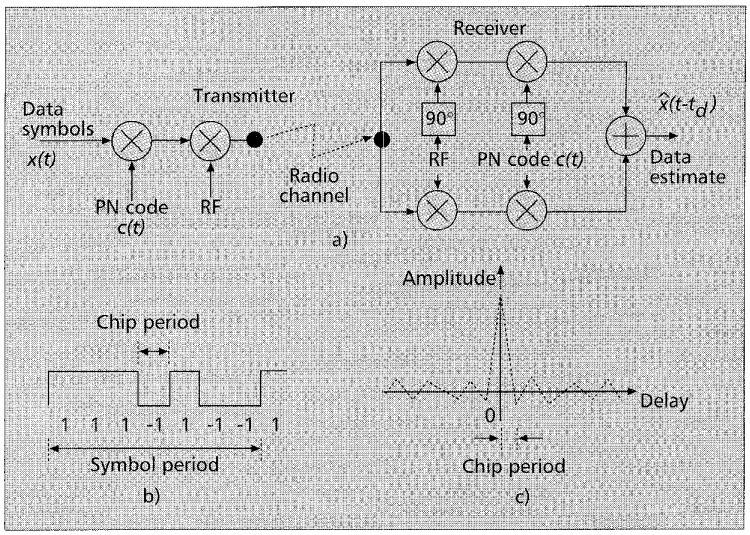

■ **Figure 1.** *a) The general form of a direct-sequence spread spectrum system; b) a typical PN code; c) a typical auto-correlation function for a PN code.*

Power Control – A corollary to the above is that power control is essential on the reverse link, to minimize multiple access interference. Otherwise, mobile transmitters far away from the cell's base station will be swamped by interference generated by users closer to the receiver. If all signals arrive with the same power, the receiver's tolerance to CDMA interference is proportional to the *processing gain* [12], $W = t_s/t_c$, where t_s is the symbol period.

The obvious way to increase the capacity of a CDMA system is to reduce the levels of multiple access interference. This may be achieved by directly canceling the interference [16] or by employing a multi-user receiver which simultaneously demodulates all users [17]. In this article, an approach based on antenna array receivers will be considered.

Why Use an Antenna Array ?

An antenna array consists of M identical[1] antenna receivers, whose operation and timing is usually controlled by one central processor. The geometry of the antenna locations can vary widely, but the most common configurations are to place the antennas around a circle (circular array) or along a straight line (linear array). Antenna arrays have frequently been proposed for the operation of radar and communications systems in a military context [18]: it is possible to perform direction finding tasks and to null out enemy interferers. However, in the context of civilian cellular systems, the aim of the antenna array receiver is purely to provide acceptable error performance and hence maximize the signal-to-interference and noise ratio (SINR) for each user in the system. An antenna array containing M elements can provide a mean power gain of M over white noise, but suppression of interference from other cellular users is dependent on the form of the received data.

A good model for the received data in a power-controlled CDMA system is a strong desired signal corrupted by a large number of small cross-correlation interference terms, which arrive with a uniform distribution from throughout the cell.[2] The array can null out $M - 1$ interferers, but for a CDMA system this is unlikely to significantly improve the received SINR [9][3] because of the very large number of interference components. In general, a better methodology is to estimate the form of the received signal and determine the matched filter solution [19]. This form of receiver can exploit any spatial diversity present, while suppressing the mean level of CDMA interference by a factor proportional to M. Assuming that the antenna array provides significantly improved SINR levels at the base station receiver, the number of channel errors, measured by the bit error ratio (BER), will reduce. This provides the cellular operator with some degrees of freedom which may be used for the following purposes [9, 20, 21]:

- To increase the number of active users for a given BER quality threshold
- To improve the BER performance for a given number of users within a cell
- To reduce the SINR required at each antenna to achieve a target BER, thus reducing the transmit power required by the mobile handset for the reverse link
- To increase the range of the base station receiver and thus the cell size
- To permit a less stringent form of reverse link power control while maintaining acceptable BER performance

While antenna arrays provide many advantages, these must be offset against the cost and complexity of their implementation. There are a number of points which must be taken into account here [22, 23]:

- The hardware/software requirements increase as M demodulators are required for each user.
- The M receivers must be accurately synchronized in time to provide effective performance.
- The computational complexity of array processing algorithms can be very large.
- The array size will be constrained by the available space for a base station. Usually, the spacing of antenna elements varies from one-half to tens of RF carrier wavelengths.

[1] *This is not strictly necessary; orthogonally polarized elements, for example, could be used instead.*

[2] *This assumption permits general results to be obtained for system capacity. However, the validity of this assumption will depend on the layout of the cell for practical situations.*

[3] *An exception is if a mobile undergoes a power control error and transmits at a very high power; nulling out the resulting interference is clearly desirable in this case.*

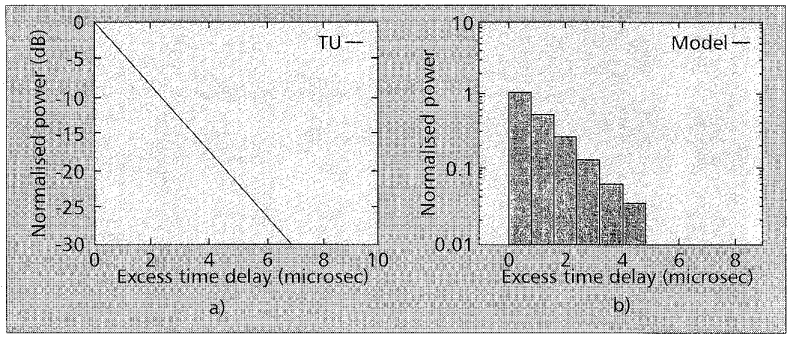

Figure 2. *a) A typical channel impulse response for an urban area; b) the discrete tap channel model.*

- Practical antenna arrays may be adversely affected by channel modeling errors, calibration errors, phase drift, and noise which is correlated between antennas.

With these points in mind, this article will move on to consider channel modeling aspects of antenna arrays. This will motivate a discussion on the likely form of a CDMA antenna array base station receiver.

Channel Modeling Considerations

In order to correctly specify the structure of an antenna array base station receiver, it is important to understand the characteristics of the radio channels that are likely to occur. There are many different types of channel model appropriate to different radio systems and scenarios, but here a channel model will be developed for a large CDMA macrocell operating in an urban environment. For simplicity, the case of a single antenna receiver will be initially considered: the results will be generalized for an antenna array receiver in the next section.

One of the most important methods for characterizing a radio channel is to determine its impulse response. This provides an indication of the severity of *multipath* propagation, which occurs due to multiple copies of the signal arriving at the receiver with different amplitudes and time delays. In dense urban areas there are many buildings and obstacles that give rise to multipath propagation, and the range of times of arrival can be significant. A typical impulse response for an urban area, drawn from the European COST-207 channel models [24], is shown in part Fig. 2a.

The correlation function of a typical CDMA code takes significant values within ±1 chip of the time of arrival of the code. This means that a CDMA correlator receiver is able to resolve multipath components of the signal which are spaced in time by 1 chip up to the symbol period. As a result, the channel impulse response measured by a CDMA receiver is often modeled by discrete channel taps [25], spaced in time by 1 PN code chip. A typical discrete tap model is shown in Fig. 2b. Each channel tap may be characterized by the following parameters: the statistical distribution of the received signal envelopes and phases, the temporal variation of each tap and the spatial variation of each tap. The symbol period for an IS-95 type system is quite high (approx. 100 μs) compared to the impulse response duration (typically a few μs), so it is commonly assumed that the number of significant channel taps $K \ll W$.

It is often assumed that each channel tap is wide-sense-stationary for the mobile moving over short distances, up to a few tens of carrier wavelengths. This means that the signal variation is due purely to phase changes in a set of independent multipath components which cannot be separated in time [26, Ch. 2]. The resolvable channel taps are assumed to be uncorrelated as each tap arises due to contributions from different multipath scatterers. The exact distributions of the signal envelopes are a function of the signal bandwidth but, for a narrowband CDMA system, two distributions are often proposed. If a dominant line of sight (LOS) path exists between the transmitter and receiver, the first received signal component will follow a Rician distribution. However, in urban areas, this is often not true: each channel tap consists of a number of independent multipath scatterers with the same probability distribution. Applying the central limit theorem, the received signal envelope statistics can be assumed to follow the Rayleigh distribution. As the mobile moves, the signal strength regularly changes by 20–30 dB: the phenomenon of a sudden loss of signal power in this context is often called *fading*.

Over a longer period of time, the average (averaged over the Rician or Rayleigh fading) received signal power levels vary according to shadowing effects, which have been found to follow a log-normal distribution. The standard deviations quoted for this distribution vary between 4–12 dB according to the type of environment encountered [27]. In addition, the average received power varies inversely with the transmitter-receiver distance R, raised to the power n. Again, the value of n varies widely, but for urban areas its value is often approximated as 4 [26, Ch. 2]. In this article, it will be assumed that power control can adequately compensate for these effects but that it is unable to compensate for Rayleigh "fast" fading: this is somewhat pessimistic compared to the quoted results for IS-95 power control systems [11].

The time variation of each channel tap depends on the motion of the mobile. As the mobile moves through spatial locations with different field strengths, each multipath component of the received signal is subject to a Doppler shift in frequency. For a CDMA signal not subject to data modulation, calculating the power spectrum of each channel tap shows the distribution of Doppler frequencies for the constituent multipaths. The maximum Doppler frequency ν_m is proportional to the vehicle speed v, according to the equation

$$\nu_m = v/\lambda \qquad (1)$$

where λ is the carrier wavelength. There are two different forms of multipath scattering, according to the excess time delay of the given channel tap [13]:

Small Excess Time Delays – The channel tap may be modeled as the accumulation of multipath components received from scatterers close to the mobile. This gives rise to the clas-

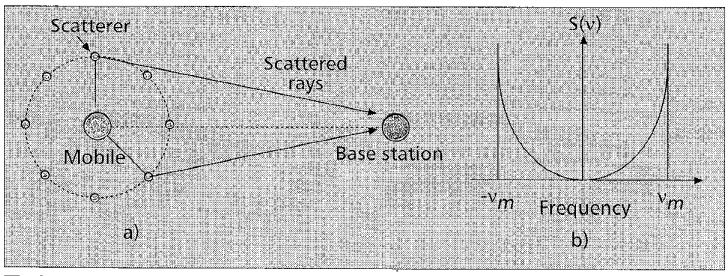

Figure 3. *The classical Doppler model: a) Geometry of multipath scattering; b) the associated Doppler power spectrum for the channel tap.*

sical Doppler power spectrum of the received multipath components, which is illustrated in Fig. 3. The equation for the Doppler power spectrum $S(\nu)$ is given by [26, Ch. 2]

$$S(\nu) = \frac{a}{1-\left(\frac{\nu}{\nu_m}\right)^2} \qquad |\nu| \le \nu_m \tag{2}$$

where ν is the Doppler frequency and a is a scaling factor.

Large Excess Time Delays – The classical Doppler model does not provide a plausible geometric model for this type of scattering. Instead, multipath energy is more likely to have a narrow Doppler spread, having arisen from reflections off isolated obstacles such as buildings or hills. One such reflection may be modeled as having a Gaussian distributed power spectrum[24], as shown in Fig. 4. The bearing of the multipath component may be determined by drawing an ellipse — sometimes called the "ellipse of Kassini" — whose major axis is the multipath length and whose foci are the transmitter and receiver [28], as shown in Fig. 4. A typical channel tap with a large time delay may comprise several such reflections.

The instantaneous variation of signal power in space for a channel tap depends on the angles of arrival of the multipath components. The distribution of multipath energy with angle has been simulated using several different methods in the literature. Lee [29] used a model based on a cosine function raised to a high power to represent the angular width (or angle spread); a Gaussian distribution of multipath energy with angle has also been used [30]. However, one of the simplest models is due to Salz and Winters [31], who use a uniform distribution of energy with angle — this model will be used for the remainder of this article. The model is shown in Fig. 5a, which shows the geometry of the model for near-in scattering. The angular width 2Δ depends on the scattering circle radius r and the distance to the base station R. The center bearing θ_0 is simply that of the mobile; for scattering with large excess time delays, a similar geometry applies replacing the circle of scatterers with the reflector giving rise to that component.

Modeling the Received Signal

In order to model a multipath channel, it will be assumed that each channel tap consists of a number of independent components. Assume that the first chip of the first channel tap for the first transmitted symbol begins to arrive at the receiver at time $t = 0$. Then the kth channel tap for the nth symbol will be detected at time $nt_s + (k-1)t_c$, where t_s and t_c are the symbol and chip periods, respectively. This tap, when measured at the output of the desired PN code correlator for a single receiver, will be denoted as

$x_1(k, nt_s + (k-1)t_c)$

and may be expanded as:

$$x_1(k, nt_s + (k-1)t_c) = d(n)\sum_{i=1}^{Q_k} A_{ki} \exp\{j(2\pi \nu_i [nt_s + (k-1)t_c] + \phi_i)\} \tag{3}$$

where Q_k denotes the number of multipaths that make up the kth tap, $d(n)$ denotes the nth transmitted symbol, and $\{A_{ki}, \nu_i, \phi_i\}$ denote the amplitude, Doppler frequency and phase of the ith multipath. In this article it will be assumed that for a fixed value of k the amplitudes A_{ki} are all equal, the phases ϕ_i are uniformly distributed over $[0, 2\pi]$ radians, and the Doppler frequencies ν_i are distributed to give the appropriate Doppler spectrum shown in Fig. 3 or 4. Equation (3) makes explicit the fact that each channel tap is a continuous function of time, although the PN code auto-correlation function means that it may only be observed once per transmitted symbol. Equation (3) assumes that $K \ll W$ so that there is no significant inter-symbol interference.

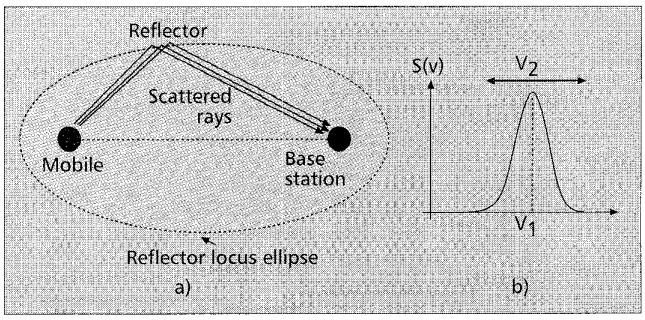

■ **Figure 4.** *a) The geometry for scattering with large excess time delays; b) the Gaussian-distributed Doppler power spectrum.*

This model can easily be extended to the case of an antenna array, using the narrowband CDMA assumption from the second section. The array will be considered to lie in the horizontal plane, with maximum length and breadth of several carrier wavelengths. In this case, each multipath arrives at all the array elements at the same time, but with an appropriate phase shift at each antenna. The form of the phase shifts is specified by the M x 1 array steering vector $\mathbf{a}(\theta)$, which may be thought of as the array response to a unit impulse arriving from bearing θ. The channel model now consists of an M x 1 vector for each channel tap: the kth channel tap vector for the nth symbol may be written as [32]:

$$\begin{aligned}\mathbf{x}(k, nt_s + (k-1)t_c) &= [x_1(k, nt_s + (k-1)t_c), x_2(k, nt_s + (k-1)t_c), \ldots, \\ &\qquad x_M(k, nt_s + (k-1)t_c)]^T \\ &= \sum_{i=1}^{Q_k} d(n) A_{ki} \exp(j2\pi\nu[nt_s + (k-1)tc] + \phi_i)\mathbf{a}(\theta_i) \\ &= d(n) A_k \mathbf{q}(k, nt_s + (k-1)t_c)\exp(\varphi_k)\end{aligned} \tag{4}$$

where θ_i denotes the bearing of the ith multipath, $x_m(k, nt_s + (k-1)t_c)$ is the channel tap output at the mth antenna, A_k denotes the signal amplitude, and $\mathbf{x}^T$ denotes the vector transpose operation. The first entry of $\mathbf{q}$ is specified to be a positive real number, so the term $\exp(\Psi_i)$ represents the carrier phase of the kth multipath at the first antenna at time t.

The statistics of a given channel tap vector $\mathbf{x}(k, t)$ are of interest. The phase of each entry of $\mathbf{x}(k, t)$ is uniformly distributed over $[0, 2\pi]$, so the mean vector of $\mathbf{x}(k, t)$ is the zero

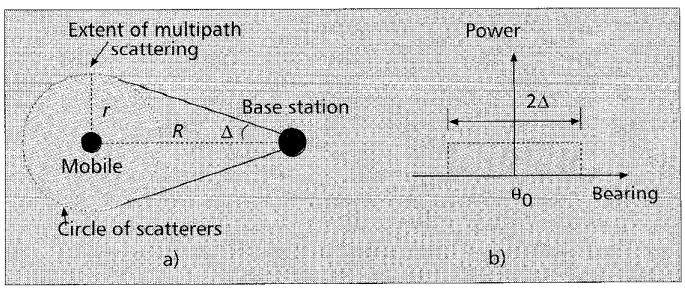

■ **Figure 5.** *a) The physical geometry for the Salz/Winters model; b) the uniform distribution of multipath energy with angle.*

vector. The second order moments of $\mathbf{x}(k, t)$ are specified by its $M \times M$ mean covariance matrix Ψ_k, which is defined as:

$$\Psi_k = E[\mathbf{x}(k,t)\mathbf{x}^H(k,t)] = \frac{A_k^2}{2\Delta}\int_{\theta_0-\Delta}^{\theta_0+\Delta}[\mathbf{a}(\phi)\mathbf{a}^H(\phi)/\mathbf{a}^H(\phi)\mathbf{a}(\phi)]\,d\phi \quad (5)$$

where E[] denotes the statistical expectation operator. The integral term arises from the fact that the distribution of multipath energy is uniform over the bearings $[\theta_0 - \Delta, \theta_0 + \Delta]$. The leading diagonal entries of this matrix specify the mean power levels of the channel tap at each antenna element; the other entries specify the cross-correlation between the channel tap signals at two different antennas.

In practice, measurements of $\mathbf{x}(k, t)$ are corrupted by three sources of interference:

- Background noise
- Auto-correlation interference from all the other taps of the given user's channel
- Cross-correlation interference from other users operating over the same bandwidth in the CDMA system

In a cellular system, the effect of the third is usually much worse than that of the first or second, and it is the limiting factor on CDMA capacity. Neglecting the first and second, the measured data vector $\mathbf{y}(nt_s + (k-1)t_c)$, of size $M \times 1$, from the antenna array at time $nt_s + (k-1)t_c$ may be written simply as the sum $\mathbf{x}(k, nt_s + (k-1)t_c) + \eta(nt_s + (k-1)t_c)$. The $M \times 1$ vector $\eta(t)$ represents the total multiple-access interference measured across the array. Initially, it will be assumed that $\eta(t)$ consists of spatially and temporally white Gaussian noise of zero mean and variance σ^2.

Signal-Combining Methods

It is clear from the previous section that the antenna array has to process a number of copies of the desired signal, each of which is corrupted by undesirable interference. If there are K significant channel taps observed at the M elements of the array, there are $K \times M$ separate data samples to be considered when making a decision on each transmitted symbol. This situation requires what is called a "multichannel" receiver, equivalent to receiving the information over $K \times M$ separate narrowband flat-fading channels. The best approach to this problem is to weight each channel appropriately and combine them together, before making a data decision. In this section, methods for combining an arbitrary number of channels will be considered; in the next section, specific receiver structures will be described.

The main difficulty in designing such a receiver is to decide how to scale each data sample before combining. Consider L multichannels, denoted as $z(l, n)$, which are to be combined. The nth sample for the lth multichannel is of the form

$$d(n)\,A_l \exp\{j\varphi_l\} + \eta l(n)$$

(consistent with the final part of Eq. (4)). Here $d(n)$ denotes the nth transmitted symbol, A_l denotes the signal amplitude, φ_l the demodulated signal carrier phase and $\eta_l(n)$ denotes all the additive interference. There are many approaches to this problem, but here four fundamental methods will be discussed [9, 33]:

Selection Diversity – If the receiver has to process a number of multichannels simultaneously, one method is simply to choose the multichannel which is presumed to have the largest signal power. This approach is quite simple, while permitting some performance improvement over single antenna receivers. However, this method does not provide the optimum improvement in SINR that can be obtained. The chosen multichannel must also be subject to data demodulation to determine $d(n)$.

Maximal Ratio Combining – If the interference observed on each separate multichannel is assumed to be uncorrelated, maximal ratio combining is the method which maximizes the SINR of the combined signals. If the interference has the same standard deviation signal for all multichannels, this method scales each signal by the complex scalar $A_l \exp\{-j\varphi_l\}$. Practical methods for estimating the carrier phases $\{\varphi_l\}$ are described in [34, Sec. 4.5]

Noncoherent Combining – If the receiver employs DPSK detection, the carrier phase reference is simply the data sample obtained for the previous symbol. The magnitude of the previous data sample also provides an estimate of the amplitude A_l, so the multichannels may be combined as follows:

$$\hat{d}(n) = \sum_{i=1}^{L} \Re\{z(i,n)z^*(i,n-1)\} \quad (6)$$

where $\hat{d}(n)$ is the estimate of the current transmitted symbol, z^* indicates the complex conjugate operation and $\Re$ denotes the real part of a complex number. As the combiner weights $z^*(i, n-1)$ are noisy, the SINR of the combined signals tends to be poorer than for maximal ratio combining. For currently used dual-diversity antennas ($L = 2$), the loss in SINR at the system operating point is typically less than 1 dB: however, as L increases the losses become greater [34, p. 302].

Wiener Filtering – The three techniques described so far are based on maximizing the signal power at the combiner output. It is also possible to use a Wiener filter, which attempts to suppress interference and maximize the SINR at the combiner output. The performance of this technique is likely to be better than that for maximal ratio combining when the interference is correlated between multichannels. This technique is discussed in more detail later.

Multichannel combiners for other modulation schemes are described in [34, Ch. 7].

Antenna Array Receiver Structures

The purpose of the antenna array receiver is to estimate the transmitted data sequence $d(n)$, based on the interference-corrupted measurements $\mathbf{y}(nt_s + (k-1)t_c)$ of the K channel taps. There are two approaches that one might consider for combining the data samples, as described below.

1D RAKE Filter – In a single antenna CDMA receiver, noncoherent combining is often used to combine the K channel taps, a method which is normally called "RAKE filtering" [15]. A simple approach to designing an antenna array receiver is to employ a RAKE filter to combine all the $K \times M$ entries of the vectors $\{\mathbf{y}(nt_s + (k-1)t_c)\}$. For DPSK modulation, this is performed using Eq. (6) with $L = K \times M$. However, as pointed out above, noncoherent combining of a lot of multichannels can give rise to large losses in SINR compared to maximal ratio combining.

2D RAKE Filter – A more effective and compact approach to dealing with the channel tap vectors $\{\mathbf{y}(nt_s + (k-1)t_c)\}$ is to apply a separate spatial filter to each tap vector in turn. The receiver can exploit any structure that might be present, such as the directions of arrival of the multipath components, their Doppler frequencies, and so on. This permits the receiver to perform coherent combining of the tap vector elements,

improving performance over the 1D RAKE filter. Denoting the kth filter as $\mathbf{h}_k$, K complex outputs are generated for the nth symbol by the vector inner products $\{\mathbf{h}_k^H \mathbf{y}(nt_s + (k-1)t_c)\}$, where $\mathbf{h}_k^H$ denotes the complex conjugate transpose operation. This means that only K outputs need to be combined using the DPSK demodulation method of Eq. (6). The approach has been called the "2D RAKE filter" because the receiver operates two separate sets of combiners in time and space. It is shown in Fig. 6: the receiver picks out the largest channel taps and selects appropriate spatial filters in each case. The outputs from the spatial filter banks are then combined in a conventional RAKE filter, ready for decision making. Base stations are frequently split into three sectors, to provide 120° coverage, which in this case corresponds to the bearings [30°, 150°] as shown.

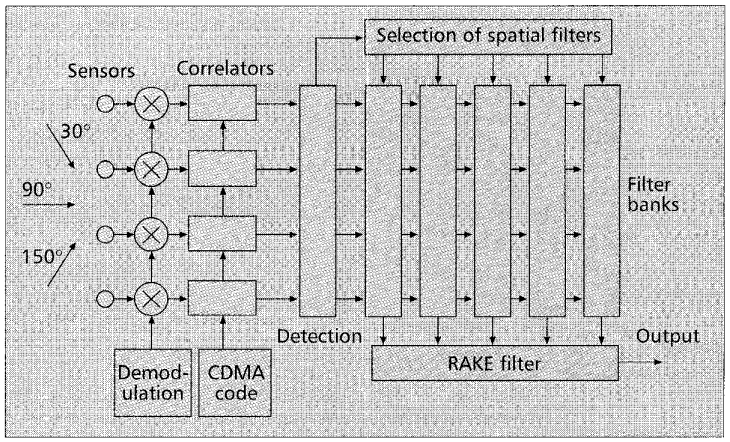

■ **Figure 6.** *The 2-D RAKE filter combiner operating in a 120° coverage sector.*

There are a number of methods to determine the form of the spatial filter $\mathbf{h}_k$. Many of these techniques employ the M x M estimated covariance matrix $\hat{\mathbf{R}}_k$ of the signal $\mathbf{y}(nt_s + (k-1)t_c)$, which is defined as:

$$\hat{\mathbf{R}}_k = \frac{1}{N}\sum_{n=1}^{N} \mathbf{y}(nt_s + (k-1)t_c)\mathbf{y}^H(nt_s + (k-1)t_c) \quad (7)$$

The notation N indicates the number of consecutive symbols used for averaging. For the chosen filter to operate effectively, the form of the array response vector $\mathbf{q}(k, nt_s + (k-1)t_c)$ should not change significantly over this time.

In this article, it will be assumed that power control ensures that the SINR of each channel tap is large enough for each vector $\mathbf{q}(k, nt_s + (k-1)t_c)$ to be correctly identified without the transmitter employing an initial training sequence. This task may be performed by blind channel identification techniques, such as:

Beamspace Transformation – This technique applies J fixed spatial filters, denoted as length M vectors $\mathbf{w}_j$, to the data [23]. By measuring the average power at the outputs, given by the product $\mathbf{w}_j^H \hat{\mathbf{R}}_k \mathbf{w}_j$, the receiver may act accordingly. A simple approach is to apply selection diversity by choosing the filter with the largest power output to pick out the desired signal.

Bearing Estimation Techniques – As the vector $\mathbf{q}(k, nt_s + (k-1)t_c)$ is composed of a number of steering vectors, it is possible to apply bearing estimation techniques to the covariance matrix $\hat{\mathbf{R}}_k$ to pick out the major directional components, as proposed in [36]. There are a number of well-known high-resolution techniques such as ESPRIT and MUSIC; however, these algorithms perform poorly in the presence of highly correlated multipath signals, which frequently occur in the urban communication channels being considered here. A simpler approach is to use the conventional beamformer (CBF) density spectrum, which is defined as:

$$P(\theta) = \mathbf{a}^H(\theta)\,\hat{\mathbf{R}}_k\,\mathbf{a}(\theta) \quad (8)$$

Again, the steering vector for the largest value of $P(\theta)$ may be selected — this approach is quite similar to *jitter diversity* [37].

Eigenfilter Techniques – In order to identify the vector $\mathbf{q}(k, nt_s + (k-1)t_c)$, it is possible to calculate the eigenvalue decomposition of $\hat{\mathbf{R}}_k$. Provided the SINR is large, the M x 1 eigenvector $\mathbf{u}_1$ corresponding to the largest eigenvalue of $\hat{\mathbf{R}}_k$ provides an estimate of $\mathbf{q}(k, nt_s + (k-1)t_c)$. This is the statistical method of principal component analysis and was used in [38].

The beamspace and bearing estimation techniques point one or more narrow beams at the incoming signals from the mobile. This choice is optimal only if each channel tap appears as a point source. If multipath scattering of the signal gives rise to a significant angular width of the signal, the performance will degrade. However, the eigenfilter method always gives weights that maximize the combiner signal power, so it should perform better in the presence of significant angular width.

If the signal power of a given tap is not significantly larger than the interference power, the above techniques are likely to incorrectly pick out an interference instead of the desired tap vector. However, given that CDMA interference generally comprises the contributions of a large number of users, it seems unlikely that any technique could correctly pick out the channel tap with sufficient SINR for the purposes of data decision making. Having noted this point, the proceeding section will now look in more detail at the operation of these blind techniques.

Algorithm Performance

In order to provide an initial comparison of these algorithms, a very simple classical Doppler one-tap channel model will be considered.[4] The receiver contains an eight-element uniform linear array (ULA), whose elements are spaced by one half of the carrier wavelength.[5] The channel tap angular width 2Δ (defined in Fig. 5) was varied from 0–60° and arrived from the array broadside, bearing 90° (i.e., perpendicular to the array, as shown in Fig. 6). Results from [31] suggest that for this bearing the signal correlation between elements falls most rapidly with the angular width 2Δ. The symbol rate of the CDMA signal was 10 ksymbols/s, and the maximum Doppler frequency was set to 0 Hz,[6] 50 Hz, or 200 Hz. The maximum achievable SINR level, defined as A_1^2/σ^2, was set to 14 dB, and N = 50 snapshots were used to estimate $\hat{\mathbf{R}}_1$. The beamspace method employed eight orthogonal spatial

[4] *Although these results are for a single tap, they provide some insight into the performance of the algorithms when they are applied to the individual channel taps of a multipath channel.*

[5] *This antenna spacing was chosen to avoid problems with the CBF bearing estimation approach. Spatial aliasing effects can occur if the antenna spacing is chosen to be much larger than half the carrier wavelength.*

[6] *In the case of 0 Hz Doppler, for each realization of the fading channel, the channel tap vector does not change over the time of observation.*

filters: the bearings were chosen as those which provided the poorest SINR for angular width $2\Delta = 0°$. As the antenna array provides a gain of 9 dB, the SINR at one antenna is 5 dB. Results from [34, p. 302] suggest that applying the 1D RAKE filter to a simple nonfading 8-multichannel scenario with each multichannel having SINR of 5 dB results in a loss of 2.5–3 dB (i.e., an SINR of 11–11.5 dB at the 1D RAKE filter output). This provides a baseline to compare the other algorithms.

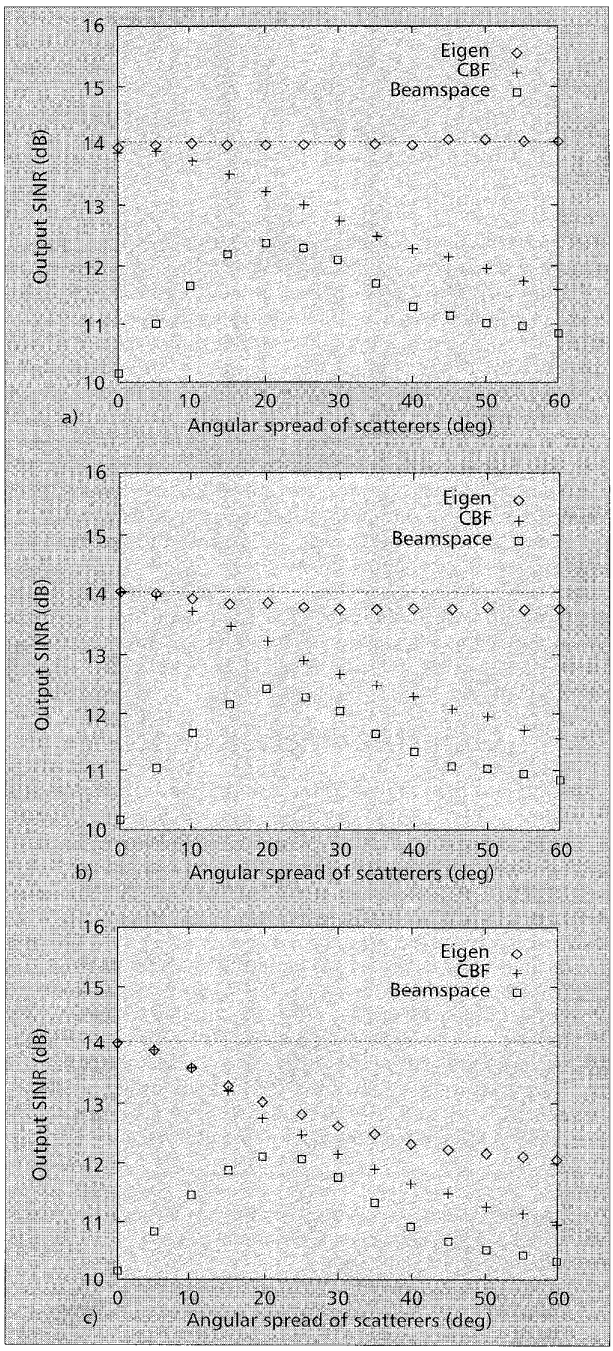

Figure 7. *The average SINR performance vs. angular width 2Δ of the beamspace, CBF and eigenfilter algorithms for maximum Doppler frequencies of a) 0 Hz; b) 50 Hz (30 mph); C) 200 Hz (120 mph).*

The average SINR at the output of the beamformers selected by the three algorithms has been determined from Monte Carlo simulations using 10,000 trials in all cases. The desired signal was generated according to Eq. (4) with $Q_k = 100$. The results for no Doppler effects (0 Hz) are shown in Fig. 7a, with a horizontal line showing the maximum attainable SINR in all cases. The results demonstrate that the eigenfilter method consistently performs well and achieves output SINR values close to the optimum. By contrast, the beamspace and CBF algorithms degrade as the angular width 2Δ increases, because the angular width of the signal energy becomes wider than the main lobe of the spatial filters $\{\mathbf{a}(\theta)\}$ — for large values of 2Δ, the performance is not much better than for the 1D RAKE technique. In the case of the beamspace technique, selecting and combining the two or three filters with the largest power levels may improve performance.

In practice, the mobile will often be in motion, giving rise to a positive Doppler frequency. The performance of the three algorithms has also been measured for Doppler frequencies of 50 and 200 Hz in Figs. 7b and 7c. Assuming the carrier frequency is 900 MHz, this corresponds to vehicle speeds of roughly 30 and 120 mph (the difference between a car moving in an urban area and someone communicating from a train). Otherwise, the simulation conditions are unchanged from before.

As the maximum Doppler frequency increases, the performance of all three techniques degrade for large multipath scattering angles. This occurs because the form of the signal vector $\mathbf{q}(k, nt_s + (k-1)t_c)$ can vary significantly as the phases of the constituent multipaths change over the sampling epoch. It is interesting to note that the performance of the eigenfilter technique degrades significantly for 200 Hz Doppler, much more so than the CBF or beamspace techniques. However, the eigenfilter approach still provides the best absolute SINR. Reducing the number of snapshots N to form $\hat{\mathbf{R}}_1$ may improve the SINR performance since the signal vector is more likely to be stationary over the sampling epoch; however, this increases the vulnerability of the algorithms to the effect of background noise.

The SINR comparison shown here between techniques based on beam-steering (i.e., the beamspace and CBF methods) and adaptive arrays (i.e., the eigenfilter approach) broadly correspond to previous published results [20]. However, no account has yet been taken here of the statistical distribution of the signal at the beamformer output, which will significantly affect the error performance of the receiver. Calculating the eigenvalues of Ψ_k defined in Eq. (5) indicates the amplitudes of the independent Rayleigh processes present in a given channel tap $\mathbf{x}(k, t)$ which can be tracked to obtain spatial diversity gain. As the probability of several independent Rayleigh processes simultaneously entering a large fade is much less than that for one Rayleigh process, the receiver is much more likely to correctly estimate the transmitted data sequence. The cumulative distribution function (CDF) indicates the likelihood of the received signal fading below a given threshold: this has been measured for the three algorithms in another Monte Carlo simulation. The simulation conditions are the same as for Fig. 7, except that the scattering width has been fixed at 20° and the maximum Doppler frequency is 0 Hz. The CDFs for the algorithms have been calculated from 100,000 trials, and the results are shown in Fig. 8. The theoretical CDF for $\mathbf{x}(k, t)$ has been calculated by substituting the eigenvalues of Ψ_k into the probability density equation [34, Eq. (7.5.26)].

The CDF for the eigenfilter is close to the optimum achievable, except at low SINRs, where the performance of the algorithm degrades slightly due to the effect of noise. Interestingly, both the CBF and beamspace approaches are able to exploit the spatial diversity of the wide angle multipath scattering, and the curves are only slightly worse than for the eigenfilter. As a result, the error performance of three algorithms may be quite similar, any difference being due to background noise effects rather than the CDF of the filter outputs.

As a contrast, the CDFs are also shown for 0° scattering and for a single fixed spatial filter placed at the source bearing. In the former case, the channel tap vector entries are completely correlated. There is no spatial diversity obtainable for this case, and the filter output follows a Rayleigh distribution. In the latter situation, the filter cannot be altered when a large fade occurs at the source bearing; indeed, it is a well-known result of multivariate statistics that the filter output will again follow a Rayleigh distribution [39]. For both curves, large fades are much more likely than for the eigenfilter, CBF or beamspace algorithms: the receiver error performance will be poor unless the SINR is very high or other multipath components are available to provide diversity.

In general, the correlation between antennas reduces as the angular width 2Δ increases or, in the case of the eigenfilter method, the antenna spacing is increased. As the mobile-to-base-station distance R increases, the value of 2Δ will generally reduce for a fixed value of the scattering radius r (Fig. 5). The available spatial diversity will reduce accordingly, so the range extension offered by antenna arrays may be affected by this factor [20].

Increasing the order of diversity produces diminishing returns in terms of the error performance of the receiver. If the decision variable CDF is measured for a receiver combining several channel taps, the improvement in the CDF due to increasing the angular width 2Δ of each tap will not be as dramatic as that shown in Fig. 8. However, some performance gain will still be obtained. The main drawback of increasing the value of 2Δ is that the correlation between the reverse and forward link channel vectors reduces [9]. If it is intended to use an antenna array to transmit to the mobiles on the forward link, using the reverse link weights for retransmission on the forward link may not be very effective. Alternative approaches such as transmission diversity [20], time division duplex reception/transmission, or transmission feedback training [40] may be more appropriate.

Another source of degradation in practice is the effect of multiple access interference. Until now, the algorithms which have been used attempt to maximize the signal power at the outputs of the combiners for the incoming channel taps. This approach maximizes the SINR when the interference is spatially and temporally white; however, if the CDMA interference does not follow this distribution, the performance of these algorithms will degrade further. In order to overcome this problem, the Wiener filtering or optimum combining techniques may be used to suppress the interference and maximise the combiner's SINR [9]. The Wiener filter solution for $\mathbf{h}_k$ may be expressed as:

$$\mathbf{h}_k = \hat{\mathbf{R}}_k^{-1}\hat{\mathbf{r}}_k \qquad (9)$$

where $\hat{r}_k$ is the cross-correlation of the desired data with $\mathbf{y}(nt_s + (k-1)t_c)$ over the N symbols. The main difficulty here is to determine the desired signal. It is possible to feedback previous decisions: however, there will be losses in performance when decision errors occur. To minimize the effects of such errors, it is possible to employ periodic training sequences, although this reduces the efficiency of the reverse link transmissions.

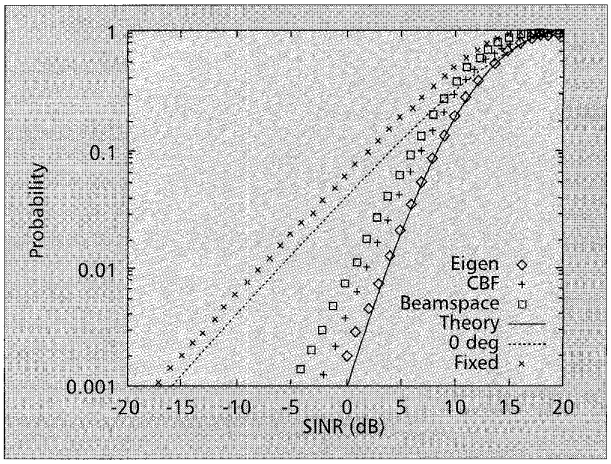

Figure 8. *The cumulative distribution functions for the beamspace, CBF, and eigenfilter algorithms, and for a fixed beamformer ("fixed") with a scattering width of 20°. The theoretical distributions for scattering widths for 20° ("Theory") and 0° ("0 deg") are also shown.*

In order to avoid training sequences a blind method for maximizing the SINR, based on the eigenfilter method, has been proposed [38]. Both pre- and post-correlation data at the receiver are used to estimate the interference covariance matrix $\hat{\mathbf{Q}}_k$. It is subtracted from $\hat{\mathbf{R}}_k$ in order to improve the estimation of the underlying signal vector $\mathbf{q}(k, t)$. The largest eigenvector $\mathbf{u}_1$ is obtained from the modified covariance matrix, and the spatial filter is given by the equation $\hat{\mathbf{Q}}_k^{-1}\mathbf{u}_1$, where $\mathbf{Q}^{-1}$ denotes the matrix inverse operation.

Performance of CDMA Antenna Arrays

The performance of antenna array base stations has been analyzed in a number of publications, including [36, 41]. Two papers have analyzed base station schemes specific to CDMA systems [19, 42]. More recently, analysis has been presented for IS-95 M-ary modulation systems [43]. In this section, the performance of a CDMA system based on the eigenfilter method and a DPSK RAKE filter will be presented, using the mean BER of a given user as a quality measure. A single-cell system will be considered with a number of active users operating over the same RF bandwidth.

The following assumptions have been made about the CDMA system:

- Each user is assumed to observe a $K = 4$ tap channel, according to the impulse response in Fig. 2. The normalized channel tap power levels $\{s_j\}$ become 0, –3, –6, and –9 dB, respectively. The channel is "slowly fading" with maximum Doppler frequency 0 Hz for each channel tap. The receiver is assumed to be able to perfectly track the desired user's channel.
- Each channel tap is corrupted by CDMA interference from all other users. Assuming that the mean power of all users is the same, the PN code filter for the desired user will suppress the power level of each other user by a factor of $3W/2$ for rectangular pulse shaping [44].
- The CDMA interference is assumed to have a uniform distribution over the range of bearings [30°, 150°]. The normalized output power γ from the desired user's spatial filter $\mathbf{h}$ for one interferer at bearing θ is simply $\mathbf{h}^H\mathbf{a}(\theta)\mathbf{a}(\theta)^H\mathbf{h}/(\mathbf{h}^H\mathbf{h})$. It is important to determine the statistical moments of γ; for example, the mean $\bar{\gamma}$ is given by:

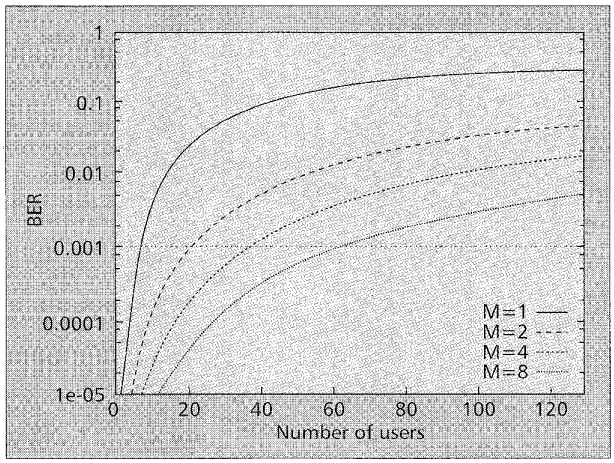

■ **Figure 9.** *The BER results plotted for different numbers of users and antenna array sizes.*

$$\bar{\gamma} = \frac{3}{2\pi}\int_{\pi/6}^{5\pi/6} (\mathbf{h}^H \mathbf{a}(\phi)\mathbf{a}(\phi)^H \mathbf{h}\, d\phi)/(\mathbf{h}^H\mathbf{h}) \qquad (10)$$

For each antenna size and scattering width, the largest value of $\bar{\gamma}$ has been selected to provide a pessimistic capacity estimate. The performance of adaptive array filters can be difficult to determine analytically, but here the power suppression level γ has been modeled as Gaussian using the central limit theorem. Its first two moments for P active users are $\bar{\gamma}\,(P-1)$ and $\bar{\gamma}^2\,(P-1)$, where $\bar{\gamma}^2$ is the covariance of γ for one interferer. As $\mathbf{h}$ always represents the matched filter for the given channel tap $\mathbf{x}(k, t)$, $\mathbf{h}$ has the zero vector as its mean vector and its mean covariance matrix is Ψ_k/A_k^2. The following steps were then used to calculate the BER performance in each case:

- The mean SINR at the spatial filter output for the jth tap is given by the equation

$$\rho_j = \frac{Ws_j}{(2/3)\gamma\sum_{k=1}^{K} s_k} \qquad (11)$$

  where s_k denotes the normalized power of the kth channel tap and the processing gain $W = 128$.
- The eigenvalues of the matrix Ψ_k indicate the number of independent Rayleigh processes at each channel tap. If there are a total of Z significant Rayleigh components for all channel taps, denote their amplitudes as $\{a_z\}$.
- Assuming that the additive interference is Gaussian distributed, zero mean, and uncorrelated between channel taps, a closed form expression for the BER may be obtained. The output of each channel tap at each antenna follows a Rayleigh distribution. The BER for a given user may be obtained by simple modification of a result from [34, Ch. 7]

$$BER = \frac{1}{2^{2K-1}}\sum_{m=0}^{K-1}\sum_{n=0}^{K-1-m}\binom{2K-1}{n}\sum_{p=1}^{Z}\frac{1}{a_p}\left(\frac{a_p}{1+a_p}\right)^{m+1}\prod_{\substack{i=1\\ i\neq p}}^{Z}\frac{a}{a_p - a_i} \qquad (12)$$

Equation (12) may be integrated over the distribution of gamma to determine the final result for each number of users.

In order to compare the performance of different antenna array sizes, Eq. (12) has been evaluated for $M = 1$, 2, 4, and 8. In each case, the maximum value of $\bar{\gamma}$ for a scattering width $2\Delta = 0.1$ has been calculated, assuming the source bearing is in the range [30°, 150°]. The results are shown for the desired user's BER vs. total number of users P in Fig. 9. In this case, the results demonstrate a significant performance improvement for a given number of users, by increasing the size of the antenna array. If a mean BER of 10^{-3} is taken as the threshold of acceptable performance, the capacity according to this measure increases from six users for one antenna to 63 for eight antenna elements. For cellular systems with a uniform distribution of users throughout the network, an additional noise term of approximately 50 percent of the single-cell CDMA interference is present. This effect will reduce the capacity by approximately 1/3; however, it can be compensated for by including error correction coding and data interleaving [11]. In addition, the system capacity may be doubled by using voice activity detection, which only permits mobile transmissions when the user is speaking; typically, one person speaks during 40 percent of a telephone conversation.

Conclusions

This article has provided an introduction to the subject of antenna arrays for narrowband CDMA base station receivers. A number of points have been discussed, and are summarized below:

- The topic of antenna arrays has been introduced, noting that they can reduce cellular interference levels and improve capacity. Results in this article suggest that employing M antennas can multiply the reverse link capacity by a factor of roughly M. However, this requires additional base station hardware and software.
- Channel modeling aspects have been described: in urban areas, several channel taps are often resolvable. Each channel tap arises geometrically through Classical Doppler or Gaussian Doppler models and has an angular width related to the distance and width of the scattering.
- The channel taps observed at antenna arrays may be modeled as the summation of array steering vectors. In urban areas, it is common for each vector entry to fade according to the Rayleigh distribution.
- The 2D RAKE filter appears to be a promising approach to handling a CDMA antenna array receiver. Several algorithms have been compared, with the eigenfilter approach performing consistently well. As the angular width of a channel tap increases, the receiver is able to exploit more spatial diversity.
- All the algorithms degrade in the presence of high Doppler frequency signals, particularly when the tap's angular width is large. In these cases, the receiver may need to employ short data lengths for channel estimation.
- The BER performance of an antenna array receiver has been estimated and significant capacity increases demonstrated. In general, the angular distribution of interference will affect the ability of a channel tap's spatial filter to suppress interference. The location of a mobile is particularly critical in determining the interference suppression levels.

There are a number of points which remain to be addressed. An important issue for antenna arrays is the scattering width of multipath components. Values have been estimated for narrowband systems (e.g., [30]), but no results appear to exist in the literature for frequency-selective CDMA systems. Efficient implementations of channel-identification algorithms are required, and more work is needed on their performance in realistic CDMA channels. The interaction of the reverse and forward links is important in practical systems, particularly to ensure that the forward link can handle the increased traffic that antenna arrays can offer on the reverse link.

Acknowledgments

This work was sponsored by EPSRC, an MOD CASE sponsorship, and Nortel Technology. The authors would also like to thank the anonymous reviewers for their helpful comments on this article.

References

[1] J. E. Padgett, C. G. Gunther, and T. Hattori, "Overview of Wireless Personal Communications," *IEEE Commun. Mag.*, vol. 33, no. 1, Jan. 1995, pp. 28–42.
[2] D. C. Cox, "Wireless Personal Communications: What Is It?" *IEEE Pers. Commun.*, vol. 2, no. 2, Apr. 1995, pp. 20–35.
[3] D. D. Falconer, F. Adachi, and B. Gudmundson, "Time Division Multiple Access Methods for Wireless Personal Communications," *IEEE Commun. Mag.*, vol. 33, no. 1, Jan. 1995, pp. 50–57.
[4] A. J. Viterbi, "The Orthogonal-Random Waveform Dichotomy for Digital Mobile Communication," *IEEE Pers. Commun.*, vol. 1, no. 1, 1st qtr., 1994, pp. 18–24
[5] C. I. Cook, "Development of Air Interface Standards for PCS," *IEEE Pers. Commun.*, vol. 1, no. 4, 4th qtr., pp. 30–34.
[6] P. G. Andermo and L.M. Ewerbring, "A CDMA-Based Radio Access Design for UMTS," *IEEE Pers. Commun.*, vol. 2, no. 1, Feb. 1995, pp. 48–53.
[7] M. Barrett and R. Arnott, "Adaptive Antennas for Mobile Communications," *IEE Elect. and Commun. Eng. J.*, vol. 5, no. 4, Aug. 1994, pp. 203–14.
[8] G. K. Chan, "Effects of Sectorization on the Spectrum Efficiency of Cellular Radio Systems," *IEEE Trans. Vehic. Tech.*, vol. 41, no. 3, Aug. 1992, pp. 217–25.
[9] J. H. Winters, J. Salz, and R. D. Gitlin, "The Impact of Antenna Diversity on the Capacity of Wireless Communication Systems," *IEEE Trans. Commun.*, vol. 42, nos. 2, 3, and 4, Feb./Mar./Apr. 1994, pp. 1740–50.
[10] J. L. Massey, "Information Theory Aspects of Spread Spectrum Communications," *Proc. 3rd IEEE Int'l. Symp. Spread Spectrum Techniques and Apps. (ISSSTA)*, Oulu, Finland, July 1994, pp. 16–21.
[11] R. Padovani, "Reverse Link Performance of IS-95 Based Cellular Systems," *IEEE Pers. Commun.*, vol. 1, no. 3, 3rd qtr., pp. 28–34.
[12] M. K. Simon *et al.*, *Spread Spectrum Communications Handbook* (Revised Ed.), New York: McGraw-Hill, 1994.
[13] W. C. Y. Lee, "Overview of Cellular CDMA," *IEEE Trans. Vehic. Tech.*, vol. 40, no. 2, May 1991, pp. 291–302.
[14] S. Haykin, *Digital Communications*, New York: John Wiley, 1988.
[15] R. Price and P. E. Green, "A Communications Technique for Multipath Channels," *Proc. IRE*, vol. 2, Mar. 1958, pp. 555–70.
[16] R. Kohno, "Spatial and Temporal Filtering for Co-Channel Interference in CDMA," *Proc. 3rd ISSSTA*, Oulu, Finland, July 1994, pp. 51–60,
[17] S. Verdu, "Adaptive Multiuser Detection," *Proc. 3rd ISSSTA*, Oulu, Finland, July 1994, pp. 43–50.
[18] B. D. Van Veen and K. M. Buckley, "Beamforming: A Versatile Approach to Spatial Filtering," *IEEE ASSP*, Apr. 1988, pp. 4–24.
[19] A. F. Naguib, A. Paulraj, and T. Kailath, "Capacity Improvement with Base-Station Antenna Arrays in Cellular CDMA," *IEEE Trans. Vehic.Tech.*, vol. 43, no. 3, Aug. 1994, pp. 691–8.
[20] J. H. Winters, "The Diversity Gain of Transmit Diversity in Wireless Systems with Rayleigh Fading," *Proc. ICC '94*, New Orleans, LA, May 1994, pp. 1121–25.
[21] A. F. Naguib and A. Paulraj, "Performance Enhancement and Trade-offs of Smart Antennas in CDMA Cellular Networks," *IEEE Vehic. Tech. Conf. (VTC)*, Chicago, IL, July 1995, pp. 40–44.
[22] S. Haykin *et al.*, "Some Aspects of Array Signal Processing," *IEE Proc.*, pt. F, vol. 139, no. 1, Feb. 1992, pp. 1–26.
[23] J. E. Hudson, *Adaptive Array Principles*, Stevenage, U.K.: Peter Peregrinus, 1981.
[24] Commission of the European Communities, "Digital Land Mobile Radio Communications: COST–207 Final Report," Ch. 2, 1988.
[25] G. L. Turin *et al.*, "A Statistical Model of Urban Multipath Propagation," *IEEE Trans. Vehic. Tech.*, vol. 21, no. 1, Feb. 1972, pp. 1–9.
[26] R. Steele (ed.), *Mobile Radio Communications*, London: Pentech Press, 1992.
[27] J. D. Parsons, *The Mobile Radio Propagation Channel*, London: Pentech Press, 1992.
[28] A. S. Bajwa and J. D. Parsons, "Small-Area Characterisation of UHF Urban and Suburban Mobile Radio Propagation," *IEE Proc.*, pt. F, vol. 129, no. 2, Apr. 1982, pp. 102–9.
[29] W. C. Y. Lee, "Effects on Correlation between Two Mobile Radio Base-Station Antennas," *IEEE Trans. Commun.*, vol. 21, no. 11, Nov. 1973, pp. 1214–23.
[30] F. Adachi et al., "Correlation between the Envelopes of 900 MHz Signals Received at a Mobile Radio Base Station Site," *IEE Proc.*, pt. F, vol. 133, no. 6, Oct. 1986, pp. 506–12.
[31] J. Salz and J. H. Winters, "Effect of Fading Correlation on Adaptive Arrays in Digital Wireless Communications," *Proc. ICC '93*, Geneva, Switzerland, May 1993, pp. 1768–74.
[32] G. Raleigh *et al.*, "Characterisation of Fast Fading Vector Channels for Multi-Antenna Communications Systems," *Proc. 28th IEEE ASIMOLAR Conf.*, Pacific Grove, CA, Nov. 1994, pp. 853–57.
[33] D. G. Brennan, "Linear Diversity Combining Techniques," *Proc. IRE*, June 1959, pp. 1075–1102.
[34] J. G. Proakis, *Digital Communications*, New York: McGraw-Hill, 1989.
[35] A. F. Naguib and A. Paulraj, "Performance of CDMA Cellular Networks with Base-Station Antenna Arrays," *Proc. Int'l. Zurich Seminar on Digital Commun.*, 1994.
[36] S. Anderson *et al.*, "An Adaptive Array for Mobile Communications Systems," *IEEE Trans. Vehic. Tech.*, vol. 40, no. 1, Feb. 1991, pp. 230–36.
[37] C. Farsakh and J. A. Nossek, "Application of Space Division Multiple Access to Mobile Radio," *Proc. 5th IEEE Int'l. Symp. Personal Indoor and Mobile Communications (PIMRC)*, The Hague, Holland, Sept. 1994, pp. 1736–39.
[38] B. Suard, *et al.*, "Performance of CDMA Mobile Communication Systems Using Antenna Arrays," *Proc. IEEE Int'l. Conf. Acoustics, Speech and Signal Processing (ICASSP)*, Minneapolis, MN, Apr. 1993, pp. IV 153–56.
[39] R. J. Muirhead, *Aspects of Multivariate Statistical Theory*, New York: Wiley, 1982.
[40] D. Gerlach and A. Paulraj, "Adaptive Transmitting Antenna Arrays with Feedback," *IEEE Sig. Processing Letts.*, vol. 1, no. 10, Oct. 1994, pp. 50–52.
[41] S. C. Swales *et al.*, "The Performance Enhancement of Multibeam Adaptive Base Station Antennas for Cellular Land Mobile Radio Systems," *IEEE Trans. Vehic. Tech.*, vol. 39, no. 1, Feb. 1990, pp. 56–67.
[42] J. C. Liberti and T. S. Rappaport, "Analytical Results for Capacity Improvements in CDMA," *IEEE Trans. Vehic. Tech.*, vol. 43, no, 3, Aug. 1994, pp. 680–90.
[43] A. F. Naguib and A. Paulraj, "Performance of DS/CDMA with M-ary Orthogonal Modulation Cell Site Antenna Arrays," *Proc. ICC '95*, Seattle, WA, June 1995, pp. 697–702.
[44] R. Meidan, R. Kohno, and L. B. Milstein, "Spread Spectrum Access Methods for Wireless Communications," *IEEE Commun. Mag.*, vol. 33, no. 1, Jan. 1995, pp. 58–67, Jan. 1995.

Biography

JOHN S. THOMPSON [M] received his B.Eng. and Ph.D. degrees from the University of Edinburgh, Scotland, in 1992 and 1996, respectively. He is currently working as a research associate at the electrical engineering department of the University of Edinburgh. His research interests include signal processing and smart antenna techniques for wireless communications. He is an associate member of the Institution of Electrical Engineers (IEE). His email address is jst@ee.ed.ac.uk.

Peter M. Grant [F] received the B.Sc. degree in electronic engineering from the Heriot-Watt University, Edinburgh, Scotland, in 1966, and the Ph.D. degree from the University of Edinburgh in 1975. He worked in radiocommunications for the Plessey Company, before he was appointed to a research fellowship at the University of Edinburgh. He was subsequently appointed to a lectureship and promoted through to a full professor of Electronic Signal Processing. During academic year 1977–78, he was the recipient of a James Caird Travelling Scholarship and, as a visiting professor, did research at the Ginzton Laboratory, Stanford University. In 1985–86 he was appointed as a visiting staff member at the MIT Lincoln Laboratory. He is a fellow of the IEE. His email address is pmg@ee.ed.ac.uk.

Bernard Mulgrew [M] received his B.Sc. degree in 1979 from Queen's University, Belfast, Ireland. After graduation he worked for four years as a development engineer in the Radar Systems Department at GEC-Marconi Avionics, Edinburgh. From 1983 to1986 he was a research associate in the Department of Electrical Engineering at the University of Edinburgh, studying the performance and design of adaptive filter algorithms. He received his Ph.D. in 1987 and is currently a senior lecturer in the department, where he gives courses on signals and systems, and signal processing. His research interests are in adaptive signal processing and estimation theory and in their application to radar and communications systems. His email address is bernie@ee.ed.ac.uk.